









ELECTRON DENSITIES IN JUPITER’S POLAR REGIONS FROM THE IDENTIFICATION OF ORDINARY–MODE WAVE CUTOFFS

A. H. Sulaiman^{1*} , O. Santolík^{2,3} , F. Allegrini^{4,5} , W. S. Kurth⁶ ,
R. L. Lysak¹ , S. S. Elliott¹ , J. D. Menietti⁶ , and S. J. Bolton² 

*Corresponding author: asulai@umn.edu

Citation:

Sulaiman et al., 2023, Electron densities in Jupiter’s polar regions from the identification of Ordinary–mode wave cutoffs, in *Planetary, Solar and Heliospheric Radio Emissions IX*, edited by C. K. Louis, C. M. Jackman, G. Fischer, A. H. Sulaiman, P. Zucca, published by DIAS, TCD, pp. 285–292, doi: 10.25546/103098

Abstract

The electron density is a critical parameter for understanding auroral processes; namely, electron acceleration via Alfvénic dissipation, electrostatic acceleration, as well as the generation and propagation of radio and plasma waves. Inferring electron densities using plasma wave spectra at the polar–most regions of Jupiter is complicated by very intense low–frequency plasma wave emissions obscuring the low–frequency cutoff, i.e., the electron plasma frequency, of the ordinary–mode waves that are routinely observed in the sub–auroral and main auroral latitudes. Furthermore, low signal–to–noise ratios and count rates hinder the derivation of electron densities from plasma moments poleward of the diffuse aurora. Here, we introduce a new technique, whereby the E/cB spectra can be utilized to reveal the Ordinary–mode wave’s cutoff, enabling accurate constraints on the electron densities at latitudes poleward of the main emission.

¹ *Minnesota Institute for Astrophysics, School of Physics and Astronomy, University of Minnesota, Minnesota, USA*

² *Department of Space Physics, Institute of Atmospheric Physics of the Czech Academy of Sciences, Prague, Czechia*

³ *Faculty of Mathematics and Physics, Charles University, Prague, Czechia*

⁴ *Southwest Research Institute, San Antonio, TX, USA*

⁵ *Department of Physics and Astronomy, University of Texas at San Antonio, San Antonio, TX, USA*

⁶ *Department of Physics and Astronomy, University of Iowa, Iowa City, IA, USA*

1 Introduction

One of the major discoveries from the Juno mission is the prevalence of broadband electron energization that accounts for Jupiter's brightest auroras (Mauk et al., 2017, 2018). This represented a shift in the paradigm of jovian auroral acceleration, long thought to be the consequence of a steady-state coupling between the magnetosphere and ionosphere (e.g., Hill, 1979; Cowley & Bunce, 2001). Terrestrial observations have underpinned the association of broadband electron energization associated with Alfvénic acceleration processes (e.g., Chaston et al., 2008). Monoenergetic energization in the form of inverted-V energy spectra is occasionally observed (Allegrini et al., 2020; Clark et al., 2018; Mauk et al., 2020; Salveter et al., 2022). Although monoenergetic distributions are commonly attributed to quasi-static currents, Alfvén waves have been shown to be capable of driving such features and generating double layers (Streltsov et al., 1998; Chaston et al., 2007). Alfvén waves are therefore thought to be important drivers of Jupiter's aurora.

Jupiter's auroral zones have been classified into three distinct zones using energetic electron spectra measured by the Jupiter Energetic-Particle Detector Instrument (JEDI; Mauk et al., 2020). The main auroral emission comprises two distinct zones, namely: (i) Zone-I which is characterized by intense electron intensities within the downward loss cones, and (ii) Zone-II which is characterized by intense electron intensities within the upward loss cones but often accompanied by equally intense electron intensities within the downward loss cones capable of causing observable and powerful auroral intensities. Zone-I and Zone-II have been demonstrated to support the upward and downward field-aligned currents, respectively (Kotsiaros et al., 2019; Mauk et al., 2020; Sulaiman et al., 2022). The third zone is the Diffuse Aurora which is equatorward of Zone-I and not the focus of this study (Li et al., 2017, 2021; Sulaiman et al., 2022).

Near-continuous constraints on the electron densities have been made on the auroral and sub-auroral latitudes using Juno observations. Plasma waves propagating in the whistler mode enabled indirect measurements of electron densities from identification of the electron plasma and lower hybrid frequencies (Elliott et al., 2021). Electron partial densities have been measured using plasma particle measurements from the Jovian Auroral Distributions Experiment (JADE; Allegrini et al., 2021). These measurements were made in the diffuse aurora up to the equatorward edge of the main emission (or Zone-I). Continuous measurements into Zone-I were made possible due to the identification of Ordinary-mode waves, which have a clear low-frequency cutoff at the electron plasma frequency f_{pe} (Sulaiman et al., 2022). Poleward of Zone-I, challenges arise in both the plasma particle-measuring technique where the signal-to-noise ratio and count rates are too low and the plasma wave-measuring technique where the f_{pe} cutoff is washed out by intense low-frequency turbulence. The polar caps have been reported to be depleted of ions (Pollock et al., 2020), however the densities of electrons remain unclear although they are expected to be comparably low.

Juno observations have thus far revealed that low-altitude flux tubes mapping to Zone-I are significantly depleted and exhibit a large variability in electron densities ranging from 0.01 to 1 cm^{-3} (Sulaiman et al., 2022). These so-called auroral cavities are inextricably linked to auroral acceleration processes (e.g., Persoon et al., 1988; Chaston et al., 2006).

A parallel electric field (not present in the ideal Alfvén wave) develops when the finite electron mass is taken into account (Goertz & Boswell, 1979). In the inertial regime, representative of Jupiter's high-latitude region, i.e., the cold electron limit, this parallel electric field becomes important on perpendicular scales of the electron inertial length, $\lambda_e = c/2\pi f_{pe}$. The plasma frequency f_{pe} is related to the electron number density, n_e , as $f_{pe} [Hz] = 8980\sqrt{n_e} [cm^{-3}]$ – the factor 8980 derived from the permittivity of free space, electron mass and charge. The parallel electric field on auroral field lines thus anti-correlates with electron density. Such a rapid decrease in density can partially reflect Alfvén waves and set up a cavity resonator whereby phase mixing enhances the parallel electric field by reducing the perpendicular wavelength of the Alfvén waves (Lysak et al., 2021). Low densities are also conducive to the generation of auroral radio waves. The Cyclotron Maser Instability requires $f_{pe}/f_{ce} \ll 1$ in the presence of a positive gradient in the perpendicular velocity distribution of weakly relativistic electrons (Wu & Lee, 1979; Louarn et al., 2017, 2018).

In this paper, we introduce a new technique that circumvents the challenge of identifying the Ordinary-mode f_{pe} cutoff in the presence of intense auroral plasma waves, enabling measurements of the electron density poleward of Zone-I (i.e, Zone-II and potentially the polar cap) thereby enhancing the latitudinal coverage. We preliminarily find the electron densities to remain low within and poleward of Zone-II and are comparable to or lower than the densities of Zone-I.

2 Technique

The Waves instrument measures an electric field component, E , using a 4.8 m tip-to-tip electric dipole antenna that is parallel to the spacecraft y -axis (Kurth et al., 2017). Its containment within the spin (x - y) plane means two electric field components are effectively measured twice per spin with a period of 30 seconds. A magnetic search coil measures a magnetic field component, B , using a single sensor mounted along the spacecraft's spin (z) axis. Signals from the antennas and search coil are both processed by a Low Frequency Receiver over a frequency range of 50 Hz – 20 kHz, providing simultaneous E - and B -field spectral densities.

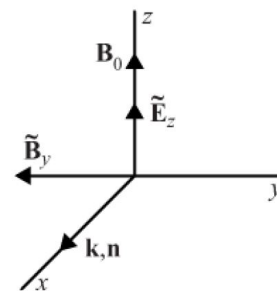


Figure 1: The electric and magnetic field eigenvectors for the Ordinary (O) mode. Adapted from Gurnett & Bhattacharjee (2005)

The Ordinary (O-) mode wave arises as one of the two roots of the dispersion relation for a cold magnetized plasma and for propagation perpendicular to the background magnetic field (the other being the Extraordinary (X-) mode). This electromagnetic wave has an electric field that is linearly polarized and parallel to the background magnetic field, \mathbf{B}_0 , and a magnetic field that is perpendicular to \mathbf{B}_0 . These fields fluctuate transverse to the direction of propagation. Figure 1 illustrates the eigenvectors of the O-mode.

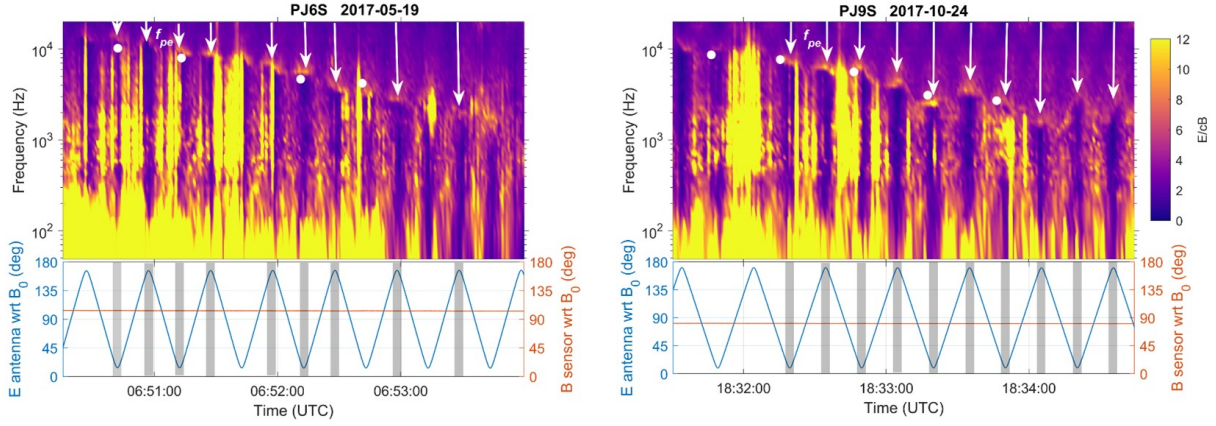


Figure 2: Spectrograms of E/cB for two events during which Juno crossed auroral magnetic field lines, during the 6th (PJ6S) and 9th (PJ9S) perijoves. Overlaid are f_{pe} derived from 30-second averaged electron partial densities measured by JADE (white circles). The low-frequency cutoff of the Ordinary mode exhibits an enhancement in E/cB and is modulated by the spacecraft spin (indicated by white arrows). Analysis of the electric field antenna angle with respect to \mathbf{B}_0 (blue curve) reveals the enhancements occur during a near-parallel orientation (gray shade regions), while the magnetic search coil angle with respect to \mathbf{B}_0 (red curve) is near-perpendicular. Altogether, these are consistent with the Ordinary mode's eigenvectors.

The dispersion relation of the O-mode is identical to that of a transverse mode in a cold unmagnetized plasma. The wave number and phase speed are respectively given by

$$k = \pm \frac{1}{c} \sqrt{\omega^2 - \omega_{pe}^2} \quad (1)$$

$$v_p = \frac{\omega}{k} = \frac{c}{\sqrt{1 - \frac{\omega_{pe}^2}{\omega^2}}} \quad (2)$$

A real wave number can only exist for $|\omega|$ above a cutoff frequency ω_{pe} (or $2\pi f_{pe}$), the electron plasma frequency. Correspondingly, at the cutoff frequency, the phase speed will diverge.

To relate the phase speed to measured E - and B -field fluctuations, we consider Fourier's representation of Faraday's law, which is given by $i\mathbf{k} \times \tilde{\mathbf{E}} = -(-i\omega)\tilde{\mathbf{B}}$. From Figure 1, we can set, without loss of generality, $\tilde{\mathbf{E}} = [0 \ 0 \ \tilde{E}_z]$, $\tilde{\mathbf{B}} = [0 \ -\tilde{B}_y \ 0]$, and $\mathbf{k} = [k \ 0 \ 0]$. For a transverse mode, we therefore have $\mathbf{k} \times \tilde{\mathbf{E}} = -k\tilde{E}_z\hat{\mathbf{y}}$. The phase speed can now be expressed as a ratio of electric to magnetic field as

$$v_p = \frac{\omega}{k} = \frac{\tilde{E}_z}{\tilde{B}_y} \quad (3)$$

Note that this coordinate system does not have the same definition as the spacecraft's coordinate system defined earlier.

Figure 2 is an example of two events when Juno was sampling magnetic field lines threading the main emission. Here, we show the measured E/cB in frequency–time. Two angles are also shown: the electric field antenna with respect to \mathbf{B}_0 and the magnetic field sensor with respect to \mathbf{B}_0 (\mathbf{B}_0 is measured by the fluxgate magnetometer, Connerney et al., 2017). Overlaid on the spectrograms are 30-second averaged electron partial densities measured by JADE and converted into f_{pe} . The E/cB exhibits a sharp increase at the low-frequency cutoff of the broadband emission interpreted as the O-mode. This is in excellent agreement with the f_{pe} measured by JADE. Further, these enhancements in E/cB are modulated by the spacecraft spin; they appear and disappear when the electric field antenna is approximately parallel and perpendicular to \mathbf{B}_0 , respectively. That, together with the magnetic field sensor steadily at an angle that is approximately perpendicular to \mathbf{B}_0 , are consistent with the eigenvectors of the O-mode.

Figure 3 shows a comparison between the theoretical phase speed from Equation 2 with the measured phase speed from Equation 3, both against frequency normalized to the plasma frequency. For Equation 2, we set the plasma frequency to be that measured by JADE (so as not to assume *a priori*). For Equation 2, we take a vertical slice from Figure 2 (PJ6S) at a time when the electric field antenna is approximately parallel to \mathbf{B}_0 (and the magnetic field sensor approximately perpendicular). Both profiles are in very good agreement with one another, exhibiting the expected divergence at f_{pe} and approaching the speed of light with increasing frequency. A similar trend also exists for PJ9S. The discrepancy between the two is likely from observing an admixture of O-mode with broadband electrostatic waves, which increases the measured E . Additionally, a larger dipole effective length would decrease the measured E (Sampl et al., 2021). Altogether these analyses give confidence that the O-mode, f_{pe} , and thus n_e are correctly identified in the auroral zones.

Finally, Figure 4 demonstrates the utility of this technique. Until now, electron densities were only inferred up to Zone-I from inspection of the electric or magnetic field spectra alone, where the O-mode low-frequency cutoff is resolvable. Poleward of Zone-I, this cutoff dips to low frequencies and becomes washed out by very intense auroral emissions. However, inspection of the E/cB spectra enables this cutoff to be resolved. It should be noted that enhancements in the E/cB alone do not uniquely identify the O-mode cutoff, and the analyses described earlier should be carried out to increase confidence of correct identification.

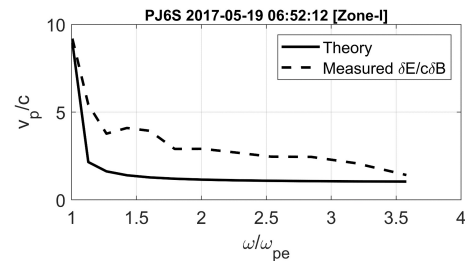


Figure 3: Theoretical (Equation 2; solid line) vs measured (Equation 3; dashed line) phase speeds. The angles between the measured $\delta\mathbf{E}$ and \mathbf{B}_0 is 13° (nearly \parallel) and between the measured $\delta\mathbf{B}$ and \mathbf{B}_0 is 103° (nearly \perp).

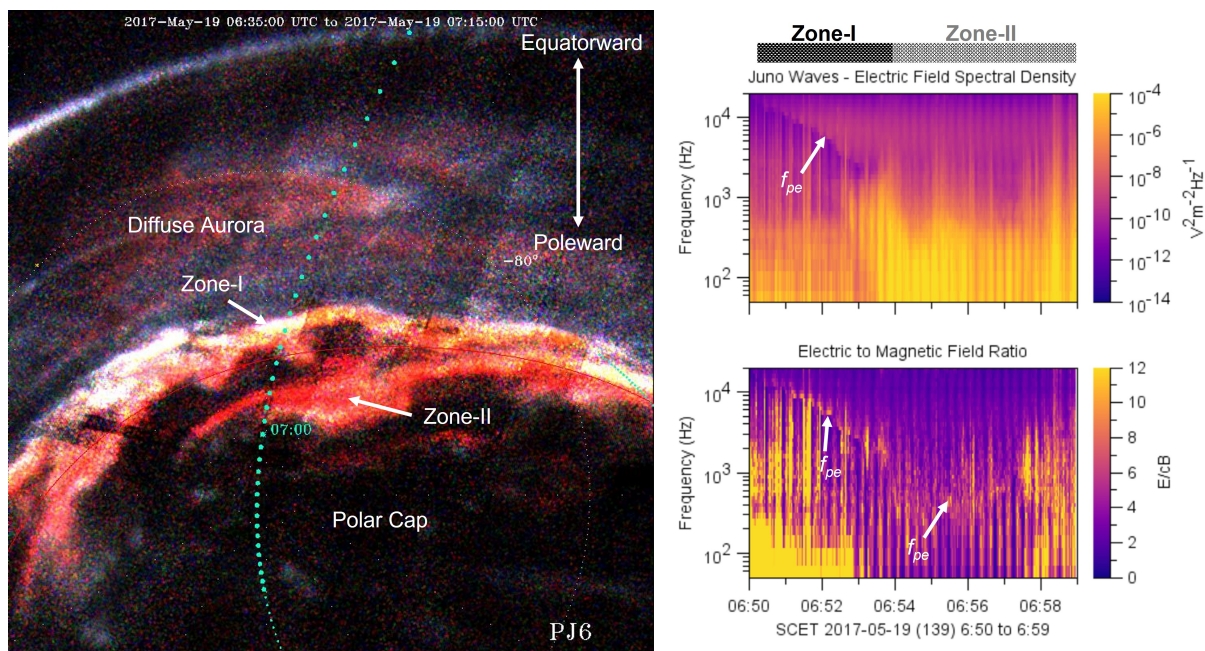


Figure 4: (Left) Annotated ultraviolet image of Jupiter’s southern aurora captured by Juno/UVS (Gladstone et al., 2017) and shown here for context. Overlaid is Juno’s magnetically mapped footprint track, spaced by one minute. (Right) Spectrograms of the electric field and the E/cB ratio. The low-frequency cutoff of the O -mode is visible in the electric field until it is washed out by intense low-frequency waves/turbulence in Zone-II. When the same event is inspected as E/cB , the low-frequency cutoff reveals itself, since this represents the phase speed which diverges at a cutoff.

3 Conclusions

Our preliminary findings show that electron densities within and poleward of Zone-II remain very low. In other words, the auroral low-density region identified in Zone-I appears to persist poleward. This is to be expected as auroral activities dominate Jupiter’s polar flux tubes. From identification of E/cB enhancements, we report preliminary electron densities in the order of 10^{-3} cm^{-3} and such numbers could indeed be necessary to produce the observed megavolt potentials formed in the polar-most regions (e.g., Clark et al., 2017). Future work will develop an electron density model in Jupiter’s polar regions. This is a necessary ingredient for the assessment of Alfvén wave dissipation, generation of potential structures, ray-tracing the propagation of plasma wave modes, and constraining source regions of auroral radio waves.

Acknowledgements

A.H.S. acknowledges G. R. Gladstone for sharing Juno-UVS images. We acknowledge the use of the Space Physics Data Repository at the University of Iowa supported by the Roy J. Carver Charitable Trust.

References

- Allegrini F., et al., 2020, Energy flux and characteristic energy of electrons over jupiter's main auroral emission, *Journal of Geophysical Research: Space Physics*, 125, e2019JA027693
- Allegrini F., et al., 2021, Electron partial density and temperature over jupiter's main auroral emission using juno observations, *Journal of Geophysical Research: Space Physics*, 126, e2021JA029426
- Chaston C., et al., 2006, Ionospheric erosion by Alfvén waves, *Journal of Geophysical Research: Space Physics*, 111, A03206
- Chaston C., Hull A., Bonnell J., Carlson C., Ergun R., Strangeway R., McFadden J., 2007, Large parallel electric fields, currents, and density cavities in dispersive alfvén waves above the aurora, *Journal of Geophysical Research: Space Physics*, 112, A05215
- Chaston C., Salem C., Bonnell J., Carlson C., Ergun R., Strangeway R., McFadden J. P., 2008, The turbulent alfvénic aurora, *Physical Review Letters*, 100, 175003
- Clark G., et al., 2018, Precipitating electron energy flux and characteristic energies in jupiter's main auroral region as measured by juno/jedi, *Journal of Geophysical Research: Space Physics*, 123, 7554
- Connerney J., et al., 2017, The juno magnetic field investigation, *Space Science Reviews*, 213, 39
- Cowley S., Bunce E., 2001, Origin of the main auroral oval in jupiter's coupled magnetosphere-ionosphere system, *Planetary and Space Science*, 49, 1067
- Elliott S., et al., 2021, The high-latitude extension of jupiter's io torus: Electron densities measured by juno waves, *Journal of Geophysical Research: Space Physics*, 126, e2021JA029195
- Gladstone G. R., et al., 2017, The ultraviolet spectrograph on nasa's juno mission, *Space Science Reviews*, 213, 447
- Goertz C., Boswell R., 1979, Magnetosphere-ionosphere coupling, *Journal of Geophysical Research: Space Physics*, 84, 7239
- Gurnett D. A., Bhattacharjee A., 2005, Introduction to plasma physics: with space and laboratory applications. Cambridge university press, doi:10.1017/CBO9780511809125
- Hill T., 1979, Inertial limit on corotation, *Journal of Geophysical Research: Space Physics*, 84, 6554
- Kotsiaros S., et al., 2019, Birkeland currents in jupiter's magnetosphere observed by the polar-orbiting juno spacecraft, *Nature Astronomy*, 3, 904
- Kurth W., et al., 2017, The juno waves investigation, *Space Science Reviews*, 213, 347

- Li W., et al., 2017, Understanding the origin of jupiter's diffuse aurora using juno's first perijove observations, *Geophysical Research Letters*, 44, 10
- Li W., et al., 2021, Quantification of diffuse auroral electron precipitation driven by whistler mode waves at jupiter, *Geophysical Research Letters*, 48, e2021GL095457
- Louarn P., et al., 2017, Generation of the jovian hectometric radiation: First lessons from juno, *Geophysical Research Letters*, 44, 4439
- Louarn P., et al., 2018, Observation of electron conics by juno: Implications for radio generation and acceleration processes, *Geophysical Research Letters*, 45, 9408
- Lysak R. L., Song Y., Elliott S., Kurth W., Sulaiman A. H., Gershman D., 2021, The jovian ionospheric alfvén resonator and auroral particle acceleration, *Journal of Geophysical Research: Space Physics*, 126, e2021JA029886
- Mauk B. H., et al., 2017, Discrete and broadband electron acceleration in jupiter's powerful aurora, *Nature*, 549, 66
- Mauk B., et al., 2018, Diverse electron and ion acceleration characteristics observed over jupiter's main aurora, *Geophysical Research Letters*, 45, 1277
- Mauk B. H., et al., 2020, Energetic particles and acceleration regions over jupiter's polar cap and main aurora: A broad overview, *Journal of Geophysical Research: Space Physics*, 125, e2019JA027699
- Persoon A., Gurnett D., Peterson W., Waite Jr J., Burch J., Green J., 1988, Electron density depletions in the nightside auroral zone, *Journal of Geophysical Research: Space Physics*, 93, 1871
- Pollock C. J., Ebert R. W., Allegrini F., Bagenal F., McComas D., Szalay J., Valek P., 2020, A persistent depletion of plasma ions within jupiter's auroral polar caps, *Geophysical Research Letters*, 47, e2020GL090764
- Salveter A., Saur J., Clark G., Mauk B., 2022, Jovian auroral electron precipitation budget—a statistical analysis of diffuse, mono-energetic, and broadband auroral electron distributions, *Journal of Geophysical Research: Space Physics*, 127, e2021JA030224
- Sampl M., Macher W., Oswald T., Plettemeier D., Rucker H. O., Kurth W. S., 2021, Juno waves high frequency antenna properties, *Radio Science*, 56, e2020RS007184
- Streltsov A., Lotko W., Johnson J., Cheng C., 1998, Small-scale, dispersive field line resonances in the hot magnetospheric plasma, *Journal of Geophysical Research: Space Physics*, 103, 26559
- Sulaiman A., et al., 2022, Jupiter's low-altitude auroral zones: Fields, particles, plasma waves, and density depletions, *Journal of Geophysical Research: Space Physics*, 127, e2022JA030334
- Wu C., Lee L., 1979, A theory of the terrestrial kilometric radiation, *The Astrophysical Journal*, 230, 621